

## HOW STRONG IS THE EVIDENCE FOR DENSITY-TRIGGERED QUENCHING?

LOUIS E. ABRAMSON<sup>1,\*</sup> AND TAKAHIRO MORISHITA<sup>1,2,†</sup>*Submitted to ApJ Letters, 26 August 2016*

## ABSTRACT

Using the deepest space-based data obtained, we find that a scenario wherein galaxy star formation is quenched by crossing a high stellar mass surface density ( $\Sigma_e \equiv M_*/2\pi r_e^2$ ) threshold is not favored over a null case where evolution from blue to red occurs at roughly fixed  $\Sigma_e$ . Two observations support this: (1) The mean  $U - V$  colors of galaxies at all  $6.5 \lesssim \log \Sigma_e / \text{M}_\odot \text{ kpc}^{-2} \lesssim 10$  have reddened since  $z \approx 3$  at rates/times correlated with  $\Sigma_e$ ; i.e., there is no preferred surface density at which blue galaxies become red, but  $\Sigma_e$  controls the pace of maturation. (2) The growth of the number of  $\log M_*/\text{M}_\odot \geq 9.4$  red galaxies at fixed  $\Sigma_e$  shows no significant enhancement over that of the global population at  $0.2 \leq z \leq 3.0$  ( $\Delta t \approx 9$  Gyr); i.e., the  $\gtrsim 2.5\times$  rise in the red fraction over that interval need not be due to blue galaxies rapidly transforming *en masse* from low to high densities, but is accounted for by the general “turning-red” of all galaxies at all  $\Sigma_e$ . These results are consistent with a scenario wherein evolutionary rates are set *ab initio* by primordial overdensities, with denser objects evolving faster than less-dense ones towards a terminal quiescence induced by gas depletion or other Hubble-timescale phenomena. Unless ruled-out by stellar ages, observed  $\Sigma_e$  thresholds are thus as likely to be consequences of density-accelerated evolution as they are causes of quenching.

*Subject headings:* galaxies: evolution — galaxies: structure

## 1. INTRODUCTION

Why some galaxies exhibit star formation while others do not is one of the central puzzles of astronomy. Quiescence correlates with mass, environment, dynamics, and structure, but whether/how these factors *cause* the cessation of star formation is unknown. The same holds for stellar mass surface density.

Non-starforming galaxies are generally denser<sup>3</sup> than contemporaneous starforming galaxies of equal mass (Holmberg 1965). Recent studies extend this finding to high- $z$  (e.g., Fang et al. 2013; Barro et al. 2013, 2015; Whitaker et al. 2016), but its meaning remains unclear.

As Lilly & Carollo (2016, hereafter LC16) discuss, there are two interpretations. The first is causal: Starforming galaxies experience dramatic increases in density due to mergers or instabilities (compaction). If such episodes drive their density into a critical range—and they are suitably massive—star formation ceases and they join the passive/quiescent/red population (Barro et al. 2015; Zolotov et al. 2015, hereafter Z15).

The second is corollary: *ab initio* denser galaxies form stars faster than less-dense ones. This accelerated evolution leads them to quiescence—the end-state for all systems—sooner, via gas exhaustion or other Hubble-timescale processes (which are rapid at high- $z$ ). Hence, non-starforming objects are by definition denser than starforming ones. This effect is amplified (or caused) by the fact that red galaxies typically reside in overdense environments, and thus assembled faster (Wechsler et al.

2006; Feldmann et al. 2016). Stellar mass surface density thus encodes accelerated evolution, but is not otherwise connected to the cessation of star formation (Holmberg 1965; Dressler 1980; Abramson et al. 2016; LC16; Morishita et al. 2016; hereafter M16).

Confirming either scenario requires establishing robust progenitor/descendant links for finely graded classes of galaxies using series of single-epoch data. This task is complicated (Behroozi et al. 2013; Kelson 2014; Abramson et al. 2016; Dressler et al. 2016), but sufficiently deep and wide data still represent powerful tests.

New *Hubble Space Telescope* (HST) imaging and spectroscopy provide these data. Surveys like the *eXtreme Deep Field* (XDF; Illingworth et al. 2013), *Grism Lens-Amplified Survey from Space* (GLASS; Treu et al. 2015), *Hubble Frontier Fields* (HFF; Lotz et al. 2016), and *Hubble Legacy Fields* (HLF; Illingworth et al. 2016) open windows into hitherto inaccessible stellar mass ranges ( $\log M_*/\text{M}_\odot \gtrsim 9$ ) at high redshifts ( $z \lesssim 3$ ), granting unprecedented leverage on the questions above.

Here, we use these data specifically to address whether galaxy stellar mass surface density causes or correlates with quiescence. Our findings in two empirical tests agree with recent modeling (LC16) to suggest that current evidence for density-triggered quenching is insufficient to favor it over a null scenario where density accelerates—as opposed to stops—galaxy evolution.

## 2. DATA

We use public XDF,<sup>4</sup> HLF,<sup>5</sup> HFF,<sup>6</sup> and GLASS data.<sup>7</sup> We take the 7-band imaging (F435, 606, 814, 105, 125, 140, 160W) covering the first four HFF cluster and parallel pointings (M16), and the 9-band imaging (HFF +

<sup>1</sup> Department of Physics & Astronomy, UCLA, 430 Portola Plaza, Los Angeles, CA 90095-1547, USA

<sup>2</sup> Astronomical Institute, Tohoku University, Aramaki, Aoba, Sendai 980-8578, Japan

\* labramson@astro.ucla.edu

† mtaka@astro.ucla.edu

<sup>3</sup> “Density” will refer to “stellar mass surface density” unless indicated otherwise.

<sup>4</sup> <https://archive.stsci.edu/prepds/xdff>

<sup>5</sup> <https://archive.stsci.edu/prepds/hlf>

<sup>6</sup> <https://archive.stsci.edu/prepds/frontier>

<sup>7</sup> <https://archive.stsci.edu/prepds/glass>

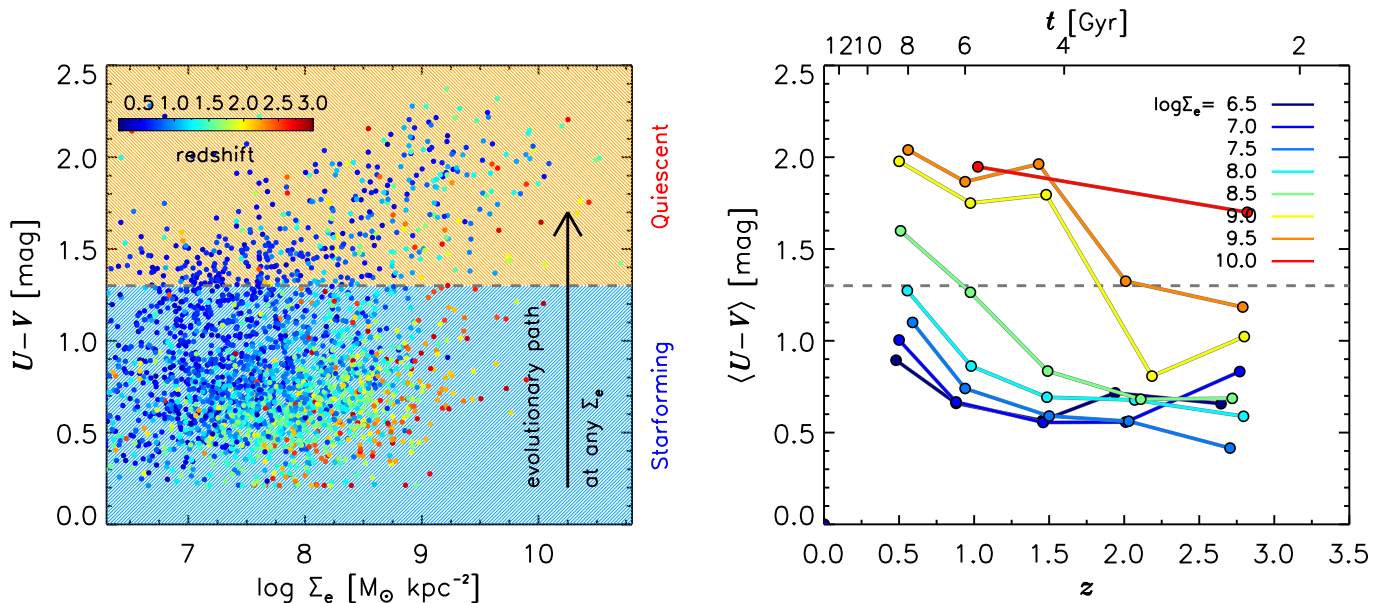


FIG. 1.— *Left*: photometric data are consistent with blue galaxies evolving into red ones at fixed mass surface density (see Holmberg 1965, Figure 6; Franx et al. 2008, Figure 6). Higher- $\Sigma_e$  objects seem to quench first, but could likewise age fastest, their natural evolution to more massive, red systems speeded by globally higher gas densities at earlier times. *Right*: the colors of galaxies at *all*  $\Sigma_e$ —to a factor of  $\sim 100$  below the Z15 quenching range—have reddened over time with the transition slowed/delayed at lower densities. No  $\Sigma_e$  quenching threshold is seen; galaxies of different densities may simply age according to different clocks (Gladders et al. 2013; Abramson et al. 2016).

F775W + 850LP) from the XDF and two HLF fields with comparable F160W data (used for structural fitting).

To prevent confounding environmental and structural effects, we exclude HFF/GLASS cluster members (M16).

Source detection and photometric redshift ( $z_{\text{phot}}$ ), rest-frame color, and stellar mass estimation are performed as in M16: EAZY (Brammer et al. 2008) determines  $z_{\text{phot}}$  using M16’s modified prior to identify cluster members; FAST (Kriek et al. 2009) provides stellar masses based on  $z_{\text{phot}}$ —or GLASS  $z_{\text{spec}}$  where possible—assuming a Chabrier (2003) IMF, Calzetti et al. (2000) dust law, and exponential star formation history. We take  $(H_0, \Omega_m, \Omega_\Lambda) = (73 \text{ km s}^{-1} \text{ Mpc}^{-1}, 0.27, 0.73)$ .

Galaxy sizes—circularized F160W effective radii;  $r_e \equiv a_e \sqrt{b/a}$ ;  $a$ ,  $b$  are semi-major and -minor axes;  $a_e$  is the half-light radius along  $a$ —derive from GALFIT (Peng et al. 2002) assuming a Sérsic (1963) profile. We study systems with  $r_e \geq \text{HWHM}_{\text{F160W}}^{\text{phys}}(z_{\text{obs}})$  ( $\text{HWHM}_{\text{F160W}}^{\text{ang}} = 0''.09$ ), which are sufficiently resolved (Morishita et al. 2014). Bright stars serve as PSFs.

We identify blue/starforming and red/non-starforming galaxies using the  $UVJ$  color-color criteria of Williams et al. (2009, their Equation 4), cutting at  $m_{\text{F160W}}^{\text{AB}} \leq 26$  where structural fits are reliable (M16). This is 1.5 mag deeper than the van der Wel et al. (2014) data. Scaling their mass completeness limit ( $\log M_*/M_\odot = 10.0$  for  $z \sim 2.5$  red galaxies), our data reach  $\log M_*/M_\odot \sim 9.4$  over  $0.2 \leq z \leq 3$ . Results are robust to this limit.

The complete sample contains 1502 (233 red + 1258 blue) galaxies.

### 2.1. A Note on $\Sigma_e$

Though some favor  $\Sigma_1$  or  $\rho_1$ —the surface or 3D stellar mass density at  $r \leq 1 \text{ kpc}$  (Fang et al. 2013; Barro et al. 2015; Whitaker et al. 2016)—we adopt  $\Sigma_e \equiv M_*/2\pi r_e^2$  because: (1) it is less sensitive to fitting errors; (2) we lack spatially resolved colors (using a global  $M_*/L$

is likely the dominant systematic; Szomoru et al. 2013; Morishita et al. 2015); (3) it avoids additional assumptions needed to infer  $\Sigma_1$  or  $\rho_1$  from 2D profiles; (4) we wish to test a null scenario where galaxies evolve at fixed density, but not fixed mass. If star formation is uniformly distributed (Nelson et al. 2015), this argues against defining “density” in a constant aperture. As a penalty, we must account for differential size/mass effects (Section 4), and verify that  $\Sigma_1$  aligns for  $\Sigma_e$ -matched progenitors/descendants (Section 3.1).

## 3. RESULTS

Figure 1, *left*, shows the data: galaxy colors as a function of stellar mass surface density— $\Sigma_e \equiv M_*/2\pi r_e^2$ —and redshift.

Starforming galaxies once occupied the entire  $\Sigma_e$  range, but have systematically vacated the high-density end as  $z \rightarrow 0$ . Conversely, high- $z$  red galaxies lie almost exclusively at the highest  $\Sigma_e$ , but appear later at lower  $\Sigma_e$ .

These statements are not inconsistent with galaxies evolving in an L-shaped track (Barro et al. 2015; Z15), increasing in density (moving right  $\rightarrow$  blue nuggets) before reaching a redshift-dependent, monotonically decreasing threshold and quenching (moving up  $\rightarrow$  red nuggets).

However, they are equally consistent with another scenario (Holmberg 1965, Figure 6) wherein blue galaxies provide a source population spanning all  $\Sigma_e$ , which is systematically emptied as they evolve at (relatively) fixed density— $d\Sigma_e/dt \ll d(U-V)/dt$  or  $ds\text{SFR}/dt$ —to end as red galaxies. If, reasonably, such evolution was fastest for the densest systems—thus the earliest, assuming galaxies encode global densities at their birth—then this “peeling” scenario would appear as threshold-triggered quenching (LC16) but entail no mechanism beyond dense gas supporting more star formation than rarefied gas (Dressler 1980; Poggianti et al. 2013b; Abramson et al. 2016; M16). We take this as a null scenario requiring falsification.

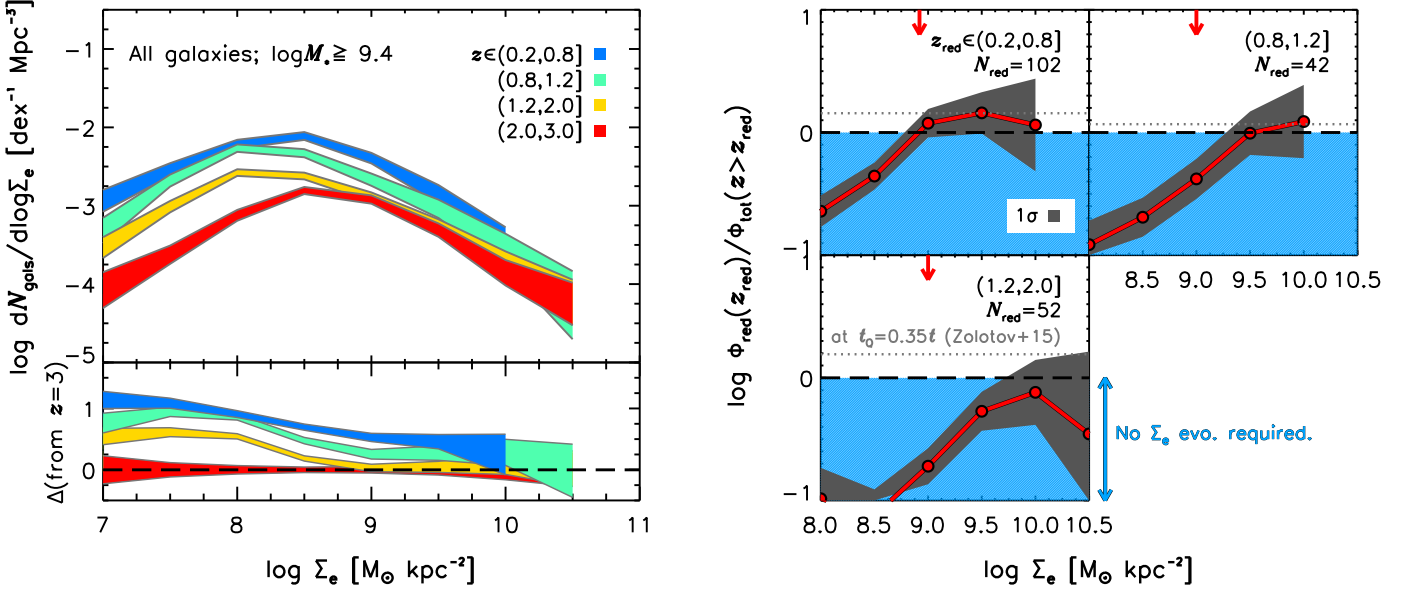


FIG. 2.— Since  $z = 3$ , galaxy counts grow mainly at lower  $\Sigma_e$ , limiting how many objects can move to higher  $\Sigma_e$  at later times (*left*; quantified at *bottom*). If such systems quenched by crossing a  $\Sigma_e$  threshold, red galaxy counts at lower  $z_{\text{red}}$  might exceed those of all equal- $\Sigma_e$ , higher- $z$  objects. The data do not suggest this (*right*). Even above published thresholds (red arrows; Whitaker et al. 2016), no significant overabundances are seen, especially when considering that  $z$ -intervals exceed a Z15 quenching time ( $t_Q = 0.35 t_z$ ), allowing galaxies to enter the sample and quench between measurements (dotted grey lines denote  $\log[(t_{z_{\text{red}}} - t_z)/t_Q]$ ; Section 3.1).

Figure 1, *right*, summarizes: The mean colors of galaxies at all surface densities have reddened with time. This process appears merely delayed or retarded for lower-compared to higher-density objects.

A mass dependence is embedded in these results in that lower- $z$  galaxies are more massive than higher- $z$  systems of equal  $\Sigma_e$ , but in some sense this is the point, signaling that galaxies might grow in mass at constant density.

Hence, Figure 1 is consistent with evolutionary rates/clocks being set by (baryonic) densities at early times ( $z > 3$ ), then remaining fixed (Gladders et al. 2013). Denser galaxies born earlier might experience the same physical processes as less-dense galaxies born later, just sooner/at accelerated rates, with no additional  $\Sigma_e$ -dependent process necessary (Kelson 2014; Papovich et al. 2015; Abramson et al. 2016; LC16).

In such a universe, apparent quenching density thresholds would still be seen and interpreted as needing to evolve (LC16; Whitaker et al. 2016). Yet, rather than a change in mechanism—an evolving quenching density—the signal would reflect the fact that all higher-density blue galaxies have peeled-off and are thus not present in lower- $z$  blue populations to support the measurement.

Since no  $\Sigma_e$  is preferred for the reddening process—which can take many Gyr (Figure 1, *right*)—a simple interpretation of the above is that there is no  $\Sigma_e$  quenching threshold. However, the data do not rule out an evolving threshold or a long quenching timescale (Section 4).

### 3.1. Abundances as Scenario Tests

So far, our results favor neither density-accelerated nor density-quenched evolution. Here, we perform a test that, while it does not dismiss the latter, would seem to increase the burden of proof.

Figure 2, *left*, shows the evolution of the  $\Sigma_e$  function—the absolute abundance of galaxies at a given surface

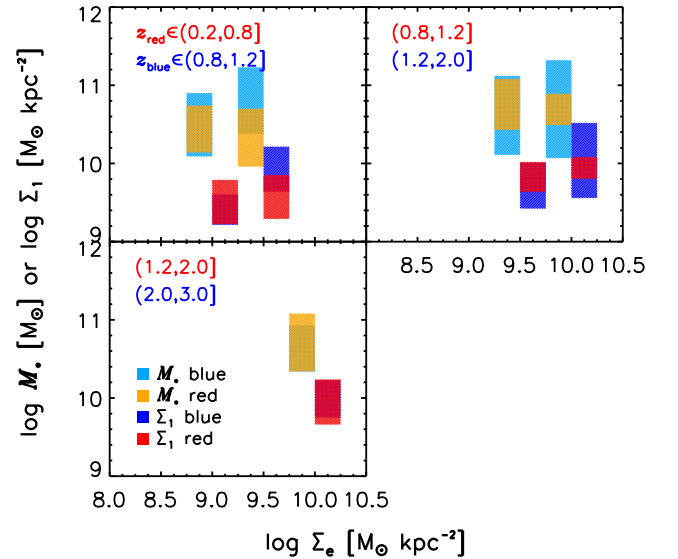


FIG. 3.— The 16<sup>th</sup>–84<sup>th</sup> pctl. ranges for  $M_*$  and  $\Sigma_1$  for blue galaxies at  $z > z_{\text{red}}$  and red ones at  $z_{\text{red}}$  overlap significantly at  $\Sigma_e$ s where quenching is prominent (Figure 2, *right*). Hence, beyond abundances, the detailed properties of many higher- $z$  blue galaxies are consistent with equal- $\Sigma_e$  red ones at later times.

density—over  $0.2 \leq z \leq 3.0$  for all galaxies with  $\log M_*/M_\odot \geq 9.4$ , the  $z \sim 3$  completeness limit. Uncertainties are the quadrature sum of Poisson error and 100 random perturbations by  $\Sigma_e$  error-bars.

In agreement with Poggianti et al. (2013a,b), at  $\sim 2\text{-}\sigma$ , nearly all  $\log \Sigma_e \gtrsim 10$  galaxies appear in-place by  $z \sim 3$ . Below that, abundances grow increasingly with decreasing  $\Sigma_e$ . This is attributable to the evolution of the blue galaxy mass function (e.g., Ilbert et al. 2010, see below), and size-mass relation (e.g., van der Wel et al. 2014; see



also LC16). Note: the slope and intrinsic dispersion of the latter allow equal- $\Sigma_e$  ( $-\Sigma_1$ ) galaxies to span factors of  $\sim 30$  (10) in  $M_*$  (Barro et al. 2015, Figure 2; M16).

With colors, we can interpret this signal to constrain the necessity of density-triggered quenching:

- **If galaxies age at fixed  $\Sigma_e$ ,** then red galaxies are the memory of once-blue ones in the same density bin. Hence, *the density function of later red galaxies should never exceed that of all earlier galaxies.* (There cannot be more descendants than progenitors.) “Earlier” means  $t < t_{\text{obs}} - t_Q$ , where  $t_Q$  is a quenching time (defined below).
- **If galaxies evolve strongly in  $\Sigma_e$ ,** then the above need not be true: previously low-density blue galaxies can compactify (Z15) to end-up as high-density red ones. Hence, *the density function of later red galaxies may exceed that of all earlier galaxies:* the red population can draw progenitors from their  $\Sigma_e$  bin and the increasingly large reservoir of lower-density systems.

Sizable overabundances of lower- $z$  red galaxies compared to all higher- $z$ , equal-density galaxies would therefore indicate compaction-/density-induced quenching.

### 3.1.1. What the Data Reveal

Following Wild et al. (2016), Figure 2, *right*, compares the red galaxy  $\Sigma_e$  functions at  $\langle z_{\text{red}} \rangle \in \{0.5, 1.0, 1.6\}$  to the total density functions at  $\langle z \rangle \in \{1.0, 1.6, 2.5\}$ . Zero is the level expected if all galaxies in a previous interval’s  $\Sigma_e$  bin quenched with no inter-interval additions. (The constant introduction of blue galaxies at many  $\Sigma_e$  hinders comparing the highest- and lowest- $z$  bins, but see below.) Under strict, constant- $\Sigma_e$  evolution, the red lines cannot lie significantly above the black dashes.

At almost all densities and times, this is what is observed.<sup>8</sup> While samples are small, at  $1-\sigma$ , red galaxies never exceed the number of older equal-density galaxies, except potentially in one of the lowest- $z$  bins.

Varying  $z$ -intervals and bin sizes, we can create  $\lesssim 2.5-\sigma$  tension at  $z < 1$ . However, if intervals are longer than a quenching time— $t_Q = 0.35 t(z) \sim 0.9\text{--}2.0$  Gyr (Z15)—galaxies can enter the sample and quench between measurements.<sup>9</sup> Indeed, red galaxy abundances only exceed those of  $z \sim 2.5$  galaxies at  $z \lesssim 0.9$ , leaving  $\gtrsim 3.5$  Gyr for this to occur. Once this is accounted for [grey dotted lines, showing  $(t_{z_{\text{red}}} - t_z)/t_Q$ ], all tension disappears.

Regarding the few bins/times where any such signal is present, “entering the sample” could mean blue galaxies evolving at constant  $\Sigma_e$  fast enough to cross the mass limit and quench without over-inflating outlier counts in the  $\Sigma_e$ – $M_*$  relation. This channel is probably sub-dominant, but could account for tens-of-percents at the relevant masses and redshifts without invoking rapid  $\Sigma_e$  evolution/quenching (Dressler et al. 2016).

Mild  $\Sigma_e$  growth could also account for it. Though it violates the strictest null scenario, a process where

$d\Sigma_e/dt \ll ds\text{SFR}/dt$  seems distinct from density-triggered quenching (Z15 Figures 2 and 3). Since  $z \sim 0.5$  red galaxies are  $\lesssim$  twice as abundant as all  $z \sim 2.5$  galaxies ( $\log \Sigma_e \geq 8$ ),  $\Sigma_e$ -bin crossing rates of  $1/\Delta t \sim 0.2 \text{ Gyr}^{-1}$  could explain the excess. This is slow compared to  $t_Q^{-1}$  (see also Poggianti et al. 2013b), except at  $z \lesssim 0.5$ , where compaction is thought to be sub-dominant for spectrophotometric reasons (Yano et al. 2016; but cf. Wild et al. 2016). Further, progenitors of (e.g.) Milky Way-mass objects grow by  $\gtrsim 10\times$  in  $M_*$  over this interval (Leitner 2012; Abramson et al. 2016), emphasizing mass- over  $\Sigma_e$ -driven quenching (see LC16; discussion of Figure 1 above).

Although abundances match, more-detailed properties of equal- $\Sigma_e$  galaxies at various times—e.g.,  $\Sigma_1$ ,  $M_*$ —might not, ruling out (quasi-)fixed-density evolution. Yet, when  $\Sigma_1$  is inferred from 1D projections of the GALFIT models, Figure 3 shows significant overlap between these quantities for earlier blue and later red galaxies at fixed  $\Sigma_e$ . So, while samples are small, no strong tension emerges at the galaxy level.

We thus find no requirement for dramatic changes in density/threshold-triggered quenching to explain the numbers/properties of red galaxies as a function of  $\Sigma_e$ : Though it may happen (Section 4), it is not obvious that the red population is built by blue galaxies jumping away from their peers towards anomalously high densities.

## 4. DISCUSSION

Amplifying Poggianti et al. (2013a,b)—whose spectroscopy demonstrates the slow evolution of the high- $\Sigma_e$  population—and LC16—whose models suggest  $\Sigma_e$  trends reflect fundamentally mass- and time-dependent physics—the results above highlight the challenge of inferring causality from correlations between galaxy mass surface density and quiescence, especially as a null hypothesis of constant- $\Sigma_e$  aging also fits the facts.

Of course, absence of evidence is not evidence of absence. Further, we do not contend that galaxies *truly* evolve at *fixed*  $\Sigma_e$ —constraints from the size-mass relation may forbid this—but that that scenario should be rejected before favoring rapid  $\Sigma_e$  growth and quenching.

The caveats of our analysis may provide ways forward.

Principally, minor mergers, adiabatic expansion, and stellar mass loss could dilute the number of observed high-density red galaxies by pushing some threshold-quenched systems back to lower  $\Sigma_e$  (Bezanson et al. 2009; Newman et al. 2012; Poggianti et al. 2013b). Simulations suggest these phenomena can lower  $\Sigma_e$  by  $\sim 10\times$  (Naab et al. 2009; Ceverino et al. 2015). Further, red galaxies are reported to grow by factors of  $\sim 3\text{--}5$  in  $r_e$  at fixed mass over the interval probed (Trujillo et al. 2007, but see below), which would also lead to large declines in  $\Sigma_e$ .

Yet, for these effects to hide threshold quenching and preserve the signal in Figure 2, *right*, the timescales must match: The flow of red galaxies out of high-density bins must balance that of blue galaxies into them. Indeed, since there are many more blue galaxies to move right than red ones to move left, the rates of density-reducing phenomena should be faster than (or tuned to) the quenching timescale. So, progenitors cannot just be dense, but must grow rapidly once quenched, perhaps tripling in size—but not mass—in the 2.5 Gyr between

<sup>8</sup>This has been interpreted as evidence for compaction and quenching (Barro et al. 2015).

<sup>9</sup>Shorter/longer  $t_Q$  will increase/decrease this leeway. The Gladders et al. (2013) model yields  $\sim 0.2 t$  (Abramson et al. 2016).

$z \sim 2$  and  $z \sim 1$  (Yano et al. 2016).

The general size-growth of red galaxies is measured across the entire redshift interval probed, so, in the mean, this process is too slow. Moreover, the null scenario of density-accelerated aging naturally explains this as the addition of lower-density red galaxies descending at later times from lower-density blue progenitors (Figure 1). Supporting this, Poggianti et al. (2013a) find red galaxies at fixed mass to grow by  $\lesssim 2\times$  once stellar age is accounted for. Given the 0.5 dex  $\Sigma_e$  bins used here, cohorts of simultaneously quenched red galaxies might thus shift one bin left, leaving our conclusions intact unless migration was a strong function of  $\Sigma_e$ .

On an individual-galaxy basis, since quenching times are short at high- $z$  ( $0.35 t < 1.5$  Gyr at  $z \gtrsim 1.5$ ), mergers and adiabatic expansion seem unlikely to drive large density reductions: there are not enough of the former and they both take too long (Newman et al. 2012; Nipoti et al. 2012; Barro et al. 2015, Figure 3). To compensate,  $t_Q$  could be raised, but at  $\gtrsim 2$  Gyr it may become difficult to disentangle  $\Sigma_e$ -triggered quenching from strangulation or gas exhaustion (e.g., Larson et al. 1980; Peng et al. 2015). If not seen as the aging “agents” in the null, fixed- $\Sigma_e$  hypothesis, these processes may be more sensitive, e.g., to environment than  $\Sigma_e$  (Wetzel et al. 2013). [Indeed,  $z \lesssim 0.6$  clusters host  $\sim 3\times$  as many dense,  $\log M_*/M_\odot \gtrsim 9$  galaxies as the field (Poggianti et al. 2013a; M16), so many high- $z$  dense objects may inhabit regions where environmental effects are non-negligible.]

Thus, rapid secular expansion seems the best out for density-triggered quenching. Since  $t_Q \gg t_{\text{dyn}}$  at  $z \lesssim 3$ , timescales would accommodate it, and simulations suggest it is possible if star formation ends in a large burst (El-Badry et al. 2016). The mechanism seems most active at  $\log M_*/M_\odot \leq 9.6$ —about a dex below most high- $z$  red galaxies—but there is some evidence at  $z \gtrsim 1.5$  and  $\log M_*/M_\odot \gtrsim 10.5$  that the largest red systems are also the *oldest* while the smallest/densest are the youngest (i.e., poststarbursts; Yano et al. 2016; O. Almaini, private communication). If confirmed using larger/deeper samples and shown not to reflect, e.g., merger-driven rejuvenations of previously red galaxies (i.e., if the poststarbursts are not too dusty), this would be a smoking gun of compaction-triggered quenching, ruling out constant-density evolution (but see LC16, Section 4). If simulations support rapid expansion, non-structural predictions such as ages would aid observers seeking to identify candidate objects and falsify hypotheses.

## 5. SUMMARY

Using the deepest HST data obtained, we show that galaxy colors, mass surface densities ( $\Sigma_e \equiv M_*/2\pi r_e^2$ ), and abundances at  $0.2 \leq z \leq 3$  and  $\log M_*/M_\odot \geq 9.4$  are consistent with a scenario in which all systems evolve from blue to red at roughly fixed  $\Sigma_e$  at rates correlated with that quantity. Though it may occur, there is no requirement that blue galaxies quench by evolving dramatically in  $\Sigma_e$  beyond a critical threshold. Specifically:

1. There is no preferred density at which blue galaxies turn red (Figure 1). Rather, this process occurs at all  $6.5 \leq \log \Sigma_e/M_\odot \text{ kpc}^{-2} \leq 10$ , with denser systems reddening earlier/faster than less-dense ones.
2. The number of red galaxies never exceeds that of all equal- $\Sigma_e$  galaxies at earlier times (Figure 2, *right*), which also have consistent masses and central-kiloparsec densities (Figure 3). There is no suggestion of a large influx of once-lower-density blue galaxies into the high-density red population.

While we cannot rule out all scenarios that might mask threshold-triggered quenching (e.g., rapid secular expansion), the most straightforward (e.g., minor mergers) seem unlikely given timescale requirements.

Thus, a simple scenario wherein galaxies evolve at roughly constant  $\Sigma_e$ , which accelerates their natural aging from blue to red via gas exhaustion or other Hubble-timescale processes—which are rapid at high  $z$ —seems equally plausible. Future investigators might falsify this/identify non-structural characteristics of galaxies undergoing threshold-triggered quenching (e.g., ages) to enable observational identification and verification of the implied mechanism(s).

We thank T. Treu, B. Poggianti, B. Vulcani, O. Almaini, D. Masters, M. Kriek, A. Wetzel, and *Galpath2016* attendees for helpful insights. T.M. acknowledges a Japanese Ministry of Education, Culture, Sports, Science and Technology Grant-in-Aid for Scientific Research (26-3871), and a Japan Society for the Promotion of Science research fellowship for young scientists. GLASS (HST-GO-13459) is supported by NASA through a grant from STScI operated by AURA under contract NAS 5-26555.

## REFERENCES

- Abramson, L. E., Gladders, M. D., Dressler, A., et al. 2016, ArXiv e-prints, arXiv:1604.00016
- Barro, G., Faber, S. M., Pérez-González, P. G., et al. 2013, ApJ, 765, 104
- Barro, G., Faber, S. M., Koo, D. C., et al. 2015, ArXiv e-prints, arXiv:1509.00469
- Behroozi, P. S., Marchesini, D., Wechsler, R. H., et al. 2013, ApJ, 777, L10
- Bezanson, R., van Dokkum, P. G., Tal, T., et al. 2009, ApJ, 697, 1290
- Brammer, G. B., van Dokkum, P. G., & Coppi, P. 2008, ApJ, 686, 1503
- Calzetti, D., Armus, L., Bohlin, R. C., et al. 2000, ApJ, 533, 682
- Ceverino, D., Dekel, A., Tweed, D., & Primack, J. 2015, MNRAS, 447, 3291
- Chabrier, G. 2003, PASP, 115, 763
- Dressler, A. 1980, ApJ, 236, 351
- Dressler, A., Kelson, D. D., Abramson, L. E., et al. 2016, ArXiv e-prints, arXiv:1607.02143
- El-Badry, K., Wetzel, A., Geha, M., et al. 2016, ApJ, 820, 131
- Fang, J. J., Faber, S. M., Koo, D. C., & Dekel, A. 2013, ApJ, 776, 63
- Feldmann, R., Hopkins, P. F., Quataert, E., Faucher-Giguère, C.-A., & Kereš, D. 2016, MNRAS, 458, L14
- Franx, M., van Dokkum, P. G., Schreiber, N. M. F., et al. 2008, ApJ, 688, 770
- Gladders, M. D., Oemler, A., Dressler, A., et al. 2013, ApJ, 770, 64
- Holmberg, E. 1965, Arkiv for Astronomi, 3, 387
- Ilbert, O., Salvato, M., Le Floc’h, E., et al. 2010, ApJ, 709, 644
- Illingworth, G., Magee, D., Bouwens, R., et al. 2016, ArXiv e-prints, arXiv:1606.00841

- Illingworth, G. D., Magee, D., Oesch, P. A., et al. 2013, *ApJS*, 209, 6
- Kelson, D. D. 2014, *ArXiv e-prints*, arXiv:1406.5191
- Kriek, M., van Dokkum, P. G., Labbé, I., et al. 2009, *ApJ*, 700, 221
- Larson, R. B., Tinsley, B. M., & Caldwell, C. N. 1980, *ApJ*, 237, 692
- Leitner, S. N. 2012, *ApJ*, 745, 149
- Lilly, S. J., & Carollo, C. M. 2016, *ArXiv e-prints*, arXiv:1604.06459
- Lotz, J. M., Koekemoer, A., Coe, D., et al. 2016, *ArXiv e-prints*, arXiv:1605.06567
- Morishita, T., Ichikawa, T., & Kajisawa, M. 2014, *ApJ*, 785, 18
- Morishita, T., Ichikawa, T., Noguchi, M., et al. 2015, *ApJ*, 805, 34
- Morishita, T., Abramson, L. E., Treu, T., et al. 2016, *ArXiv e-prints*, arXiv:1607.00384
- Naab, T., Johansson, P. H., & Ostriker, J. P. 2009, *ApJ*, 699, L178
- Nelson, E. J., van Dokkum, P. G., Förster Schreiber, N. M., et al. 2015, *ArXiv e-prints*, arXiv:1507.03999
- Newman, A. B., Ellis, R. S., Bundy, K., & Treu, T. 2012, *ApJ*, 746, 162
- Nipoti, C., Treu, T., Leauthaud, A., et al. 2012, *MNRAS*, 422, 1714
- Papovich, C., Labbé, I., Quadri, R., et al. 2015, *ApJ*, 803, 26
- Peng, C. Y., Ho, L. C., Impey, C. D., & Rix, H.-W. 2002, *AJ*, 124, 266
- Peng, Y., Maiolino, R., & Cochrane, R. 2015, *Nature*, 521, 192
- Poggianti, B. M., Moretti, A., Calvi, R., et al. 2013a, *ApJ*, 777, 125
- Poggianti, B. M., Calvi, R., Bindoni, D., et al. 2013b, *ApJ*, 762, 77
- Sérsic, J. L. 1963, *Boletin de la Asociacion Argentina de Astronomia La Plata Argentina*, 6, 99
- Szomoru, D., Franx, M., van Dokkum, P. G., et al. 2013, *ApJ*, 763, 73
- Treu, T., Schmidt, K. B., Brammer, G. B., et al. 2015, *ApJ*, 812, 114
- Trujillo, I., Conselice, C. J., Bundy, K., et al. 2007, *MNRAS*, 382, 109
- van der Wel, A., Franx, M., van Dokkum, P. G., et al. 2014, *ApJ*, 788, 28
- Wechsler, R. H., Zentner, A. R., Bullock, J. S., Kravtsov, A. V., & Allgood, B. 2006, *ApJ*, 652, 71
- Wetzel, A. R., Tinker, J. L., Conroy, C., & van den Bosch, F. C. 2013, *MNRAS*, 432, 336
- Whitaker, K. E., Bezanson, R., van Dokkum, P. G., et al. 2016, *ArXiv e-prints*, arXiv:1607.03107
- Wild, V., Almaini, O., Dunlop, J., et al. 2016, *ArXiv e-prints*, arXiv:1608.00588
- Williams, R. J., Quadri, R. F., Franx, M., van Dokkum, P., & Labbé, I. 2009, *ApJ*, 691, 1879
- Yano, M., Kriek, M., van der Wel, A., & Whitaker, K. E. 2016, *ApJ*, 817, L21
- Zolotov, A., Dekel, A., Mandelker, N., et al. 2015, *MNRAS*, 450, 2327